Far East Journal of Electronics and Communications
SASTRA Nat. Conf. Elec. Sci. Tech., 2015

http://dx.doi.org/10.17654/EC03010089
Special Issue (March, 2016), Pages 89-101 **ISSN: 0973-7006**

DWT DECOMPOSITION WITH DIFFERENT WAVELET ORDERS FOR NOISE SUPPRESSION OF ULTRASONIC B-SCAN IMAGE OF AUSTENITIC STAINLESS STEEL WELD PAD

K. Manjula, K. Vijayarekha and B. Venkatraman

School of CSE
SRC, SASTRA University
Kumbakonam 612 001, India
e-mail: manjumarsin@src.sastra.edu

School of EEE
SASTRA University
Thanjavur 613 401, India
e-mail: vijayarekha@eee.sastra.edu

Radiological Safety Group
Indira Gandhi Centre for Atomic Research
Kalpakkam 603 102, India
e-mail: bvenkat@igcar.gov.in

Abstract

Welding is a major task for any component fabrication in every industry. Irrespective of the number of years of the science and art of welding, defects may continue to occur in its lifetime or during

Received: October 24, 2015; Revised: December 17, 2015; Accepted: December 31, 2015
Keywords and phrases: coiflet, daubechies, discrete wavelet transform, symlet, time of flight diffraction.

*Corresponding author

Communicated by A. Srinivasan, Guest Editor

welding. The welds are expected to be tested and evaluated using codes of practice. Nowadays industries extensively used ultrasonic testing to detect and evaluate the defects/flaws in the weldments. Ultrasonic testing has extensive developments in the last two decades because of the advancement in sensor and signal analysis technologies. Time of flight diffraction is the advanced technique which has better probability of detection of linear defects. A major irritant during application of ToFD especially for the inspecting of austenitic stainless steel weldments is the presence of noises. Such noises have been reduced utilizing different approaches and each has its own merits and demerits. This paper focuses on the application of discrete wavelet transform (DWT) decompositions with lower-order wavelet filters for de-noising ultrasonic ToFD B-scan images. Analysis clearly indicates that this approach also gives greater SNR improvement with less computational time.

1. Introduction

Whenever an ultrasonic image acquisition process occurs, the noises may be introduced into the images. The noise can be described as an unwanted high frequency information which is randomly or repetitively distributed. Even if it is distributed randomly, its distribution is uniform over a range of spectrum. Instrumental noise is associated with the equipment that may affect acquired images. The recognizable noises such as environmental noise, flicker noise, shot noise, and thermal noise (Johnson) can be suppressed by using temporal averaging.

In ultrasonic testing, the sound wave is used to capture and characterize the defect. But the sound wave is scattered from one grain to another grain before returning to the probe. The microstructure of coarse-grained structured material is intended to be scattered during UT. This scattered noise is recognized as the material noise. This sort of noise is highly affected by the ultrasonic A-scan signals. It leads to distortion in the ultrasonic B-scan images. That is, coherent noise covers the flaw echo and thus it must be reduced by using coherent nature of frequency diversity techniques. Because of this noise, the flaw image quality can be affected. That is the noise affects

the image strengths and the reliability of the test. Therefore, it must be suppressed before identifying the presence of weld defect in the images. It can be suppressed by using various transforms.

2. Literature Survey

The authors reviewed various papers [1-7] for reducing noise from the ultrasonic image. Fourier transform, short time Fourier transform, Hough transform, wavelet transform, and split spectrum processing are known transforms and technique that are used to suppress the noise from the image. Because of the better performance of the wavelet transform, it is widely used to reduce the noise from the B-scan image.

Wavelet transform

Wavelet transform gives frequency and time information. The image has components, namely, approximation coefficients and detail coefficients across vertical, horizontal and diagonal directions in the frequency domain. An identity of the image can be captured using approximation coefficients, i.e., low frequency components of it. It is the vital part of the image. The detail coefficients of the image are known as unwanted information, i.e., noise. The ultrasound image can be decomposed into a succession of spatial resolution image using DWT decompositions. Figure 1 shows that the two-level DWT decompositions. In multi-level DWT decompositions, the approximation coefficients are to be decomposed recursively. Hence, the wavelet decomposition tree is to be obtained by breaking down the given input image into many lower resolution components.

Figure 1 shows the two-level DWT decompositions of an image. In Figure 1,

$$\text{Input image} = cA_1 + cD_{V1} + cD_{H1} + cD_{D1}$$

$$= cA_2 + cD_{V2} + cD_{H2} + cD_{D2} + cD_{V1} + cD_{H1} + cD_{D1}.$$

The approximations of input image at decomposition levels 1 and 2 are cA_1 and cA_2. The details of input image at decomposition level 1 are cD_{H1},

cD_{V1}, cD_{D1}. Similarly, details of input image of decomposition level 2 are cD_{H2}, cD_{V2}, and cD_{D2}.

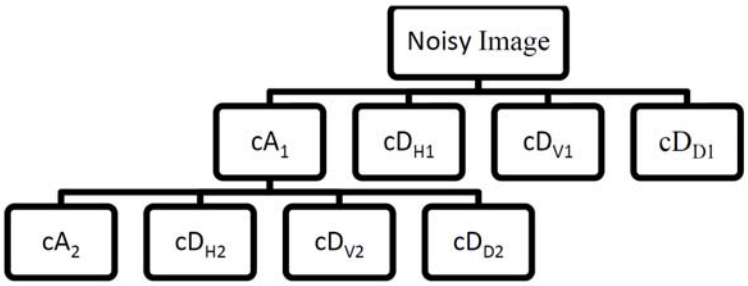

Figure 1. Two-level DWT decompositions.

Approximation coefficients (cA_i), detail coefficients across the diagonal (cD_{Di}), horizontal (cD_{Hi}) and vertical (cD_{Vi}) directions are known as the four sets of coefficients generated at each DWT decomposition levels. Figure 2 shows the process of image de-noising using three-level decompositions. Top-left sub-image at DWT decomposition level 3 is the de-noised image. Distribution of images' energy is normally located at the lower frequency band.

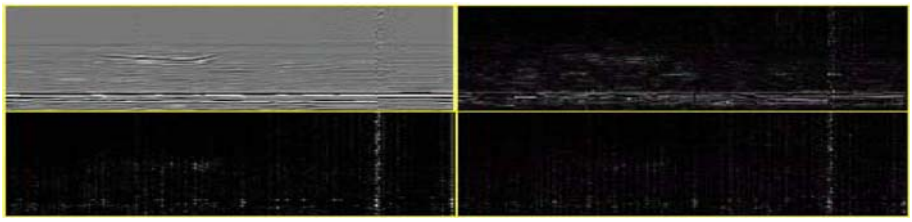

(a) DWT decomposition at level 1

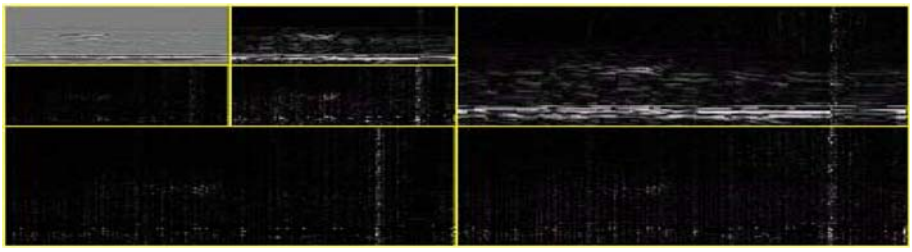

(b) DWT decomposition at level 2

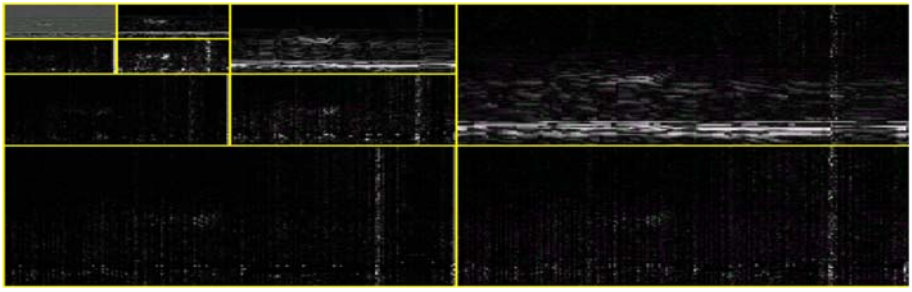

(c) DWT decomposition at level 3

Figure 2. Image de-noising using three-level DWT decompositions.

Perceptual quality

The act of perceiving the quality of an image is known as perceptual quality. Maximum Squared Error (MAXERR), Mean Square Error (MSE), Peak Signal to Noise Ratio (PSNR), and Ratio of Squared Norms (L2RAT) are the measurements used to assess the perceptual quality of an image. Out of these measurements, PSNR and MSE are commonly used to measure the perceptual quality of the image.

Mean Square Error

The MSE represents the mean squared error between the de-noised and the original image. It is calculated by:

$$MSE = \frac{1}{rc}\sum_{k=0}^{r-1}\sum_{l=0}^{c-1}[I(k,\, i) - I_d(k,\, i)]^2. \tag{1}$$

If the MSE value is lower, then the error becomes lower.

- The Peak Signal to Noise Ratio: PSNR denotes the measure of the peak error and expressed in decibels. It is defined by:

$$PSNR = 10\log_{10}\left(\frac{255^2}{MSE}\right). \tag{2}$$

If its value is high, then the quality of the de-noised image is good.

Methodology - ultrasonic time of flight diffraction technique

In ultrasonic ToFD the energy will be reflected from the defects or

surfaces of the weldment. The measurement of diffracted energy from the tips of a defect is known as ToFD technique. It provides high scanning speed, high accuracy defect sizing, etc. In it, the transmitter probe (transducer) is used to pass the ultrasonic wave over the test specimen. The wave which propagates along the top surface of the test specimen is known as lateral wave. Similarly, the wave which propagates from the bottom of the specimen is known as back-wall echo. Based on the presence of defects, the waves are diffracted. The diffracted waves from the tips of the defects are present in between both the lateral wave and the back-wall echo. These echoes are captured by the receiver probe. Every ToFD image basically contains lateral wave and back-wall echo. If the image is defective, it also contains defects echo or flaw echo.

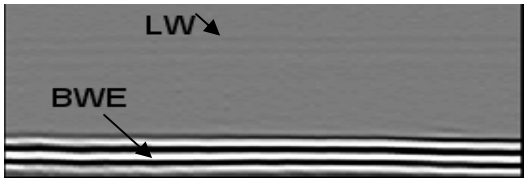

Figure 3. Ultrasonic ToFD B-scan image of ASS weld plate.

Figure 3 shows the image of the defect less B-scan image. In it, LW denotes lateral wave and BWE denotes back-wall echo. If the defect is present in the weld area, then the defect echo is also displayed in between LW and BWE of the image.

Experimental Details

In this work, MicroPlus AEA Technology's ToFD equipment is used along with the encoder. 80 dB is set as the channel gain. Figure 4 shows that the ultrasonic ToFD experiment setup for acquiring images of austenitic SS weld plate of size length × breadth × height mm. *T* denotes transmitter probe; and *R* indicates receiver probe. The parameters such as transducer's frequency (MHz), its angle and probe separation, longitudinal velocity of austenitic stainless steel (m/s), etc. must be considered in this experiment.

Using a transducer, the sound energy is converted into electrical energy and vice versa. B-scan image is captured by acquiring A-scan signals using the number of successive probe positions. The ToFD equipment is calibrated using encoder. That is, B-scan image is produced using consecutive A-scan signals. The acquired ultrasonic signal may also have echoes from noises.

Therefore, the image may have these noise echoes. These noise echoes must be reduced, i.e., image quality must be enhanced.

Figure 4. ToFD equipmental setup.

3. Result and Analysis

A 25 mm thick × 142 mm breadth × 145 mm long weld plate or pad of 304LN grade austenitic stainless steel has been fabricated by double 'V' Shielded Metal Arc Welding method. Probe separation is 33.33 mm. The slag inclusion was purposely introduced in this weld pad. Figure 5 gives the radiographic image of the specified weld plate. The image is acquired from side A to side B of the weld pad. This weld pad has been scanned by ToFD equipment. A 4 MHz, 45° longitudinal angular probe has been used to launch waves into the material. The experiment was conducted at room temperature and the equipment used was MICROPLUS from AEA Technology, UK. ToFD images have been acquired using ToFD equipment which was connected with digital encoder as shown in Figure 4. The acquired image is given in Figure 6 and it is de-noised using discrete wavelet transform with different wavelet filters (mother wavelets).

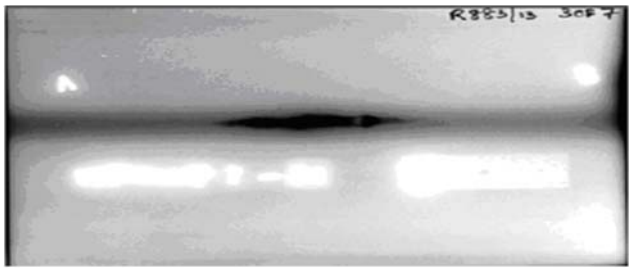

Figure 5. Radiographic image of a weld plate with slag.

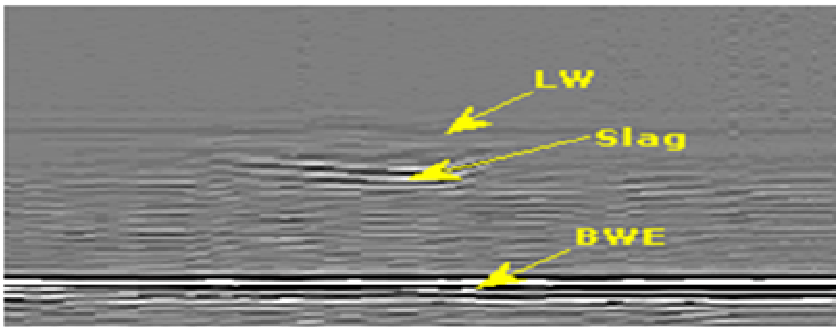

Figure 6. Before de-noising - noisy image (slag).

Figure 7 shows single-level DWT decomposition (approximation and detail) of noisy image using various wavelet filters. Peak Signal to Noise Ratio is measured in terms of decibel (dB) using equation (2). MATLAB, MS-Excel, and Yokogawa Xviewer applications are also used to get the outputs.

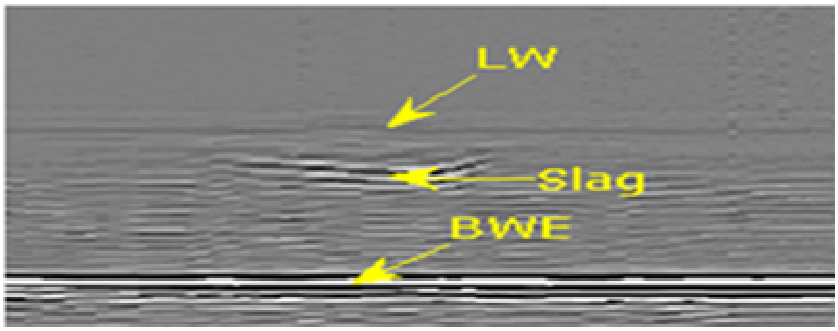

(a) Single-level decomposition with symlet filter

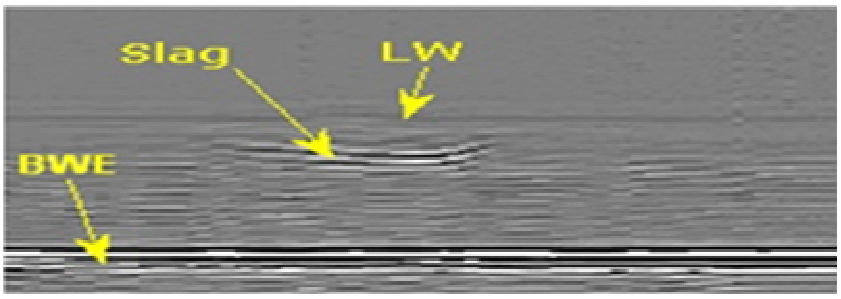

(b) Single-level decomposition with daubechies filter

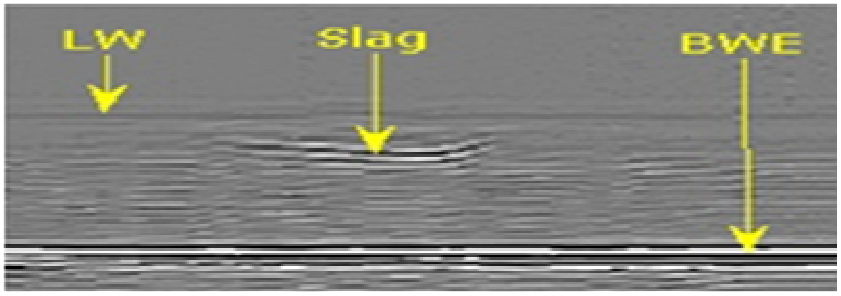

(c) Single-level decomposition with coiflet filter

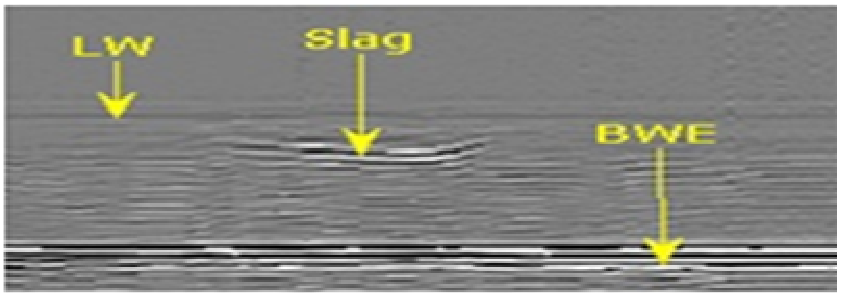

(d) Single-level decomposition with biorthogonal filter

Figure 7. After de-noising - de-noised image (slag).

The following results are concluded from Figure 8. Irrespective of DWT decomposition level, PSNR value gets increased by using coiflet wavelet filter with vanishing moments 1, 2, 3 and 4. Using wavelet filters symlet and daubechies with vanishing moments 1 upto 4, PSNR values get decreased. For db1 and sym1, the PSNR value of the de-noised image is high in decomposition level 1 and MSE value is low for the same. But for coif4 and

bior6.8, PSNR value is high when the decomposition level is 1. Irrespective of the decomposition levels, PSNR value using higher-order wavelets (i.e., wavelets with high vanishing moments – db2, db3, db4 or sym2,..) get reduced than that of db1 (sym1) whereas PSNR value gets increased for wavelet filters such as coiflet and biorthogonal. For all wavelet filters, PSNR value gets reduced when decomposition level gets increased whereas the MSE value of it gets high. Irrespective of decomposition level, PSNR value using the daubechies remains same as the symlet with vanishing moments 1, 2 and 3. The computational time is the time taken to read the image, de-noise it using DWT and display the de-noised image. Table 1 shows that the average computational time is less in decomposition level 1 than that of decomposition level 4.

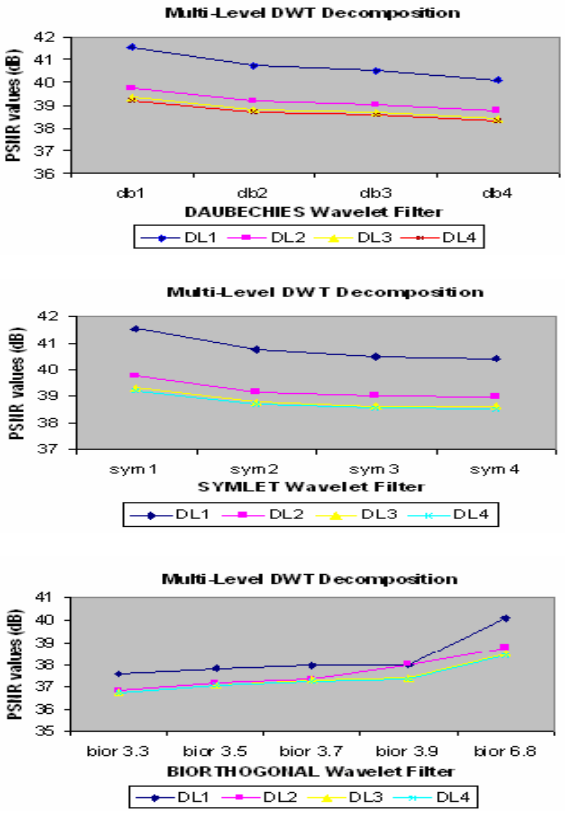

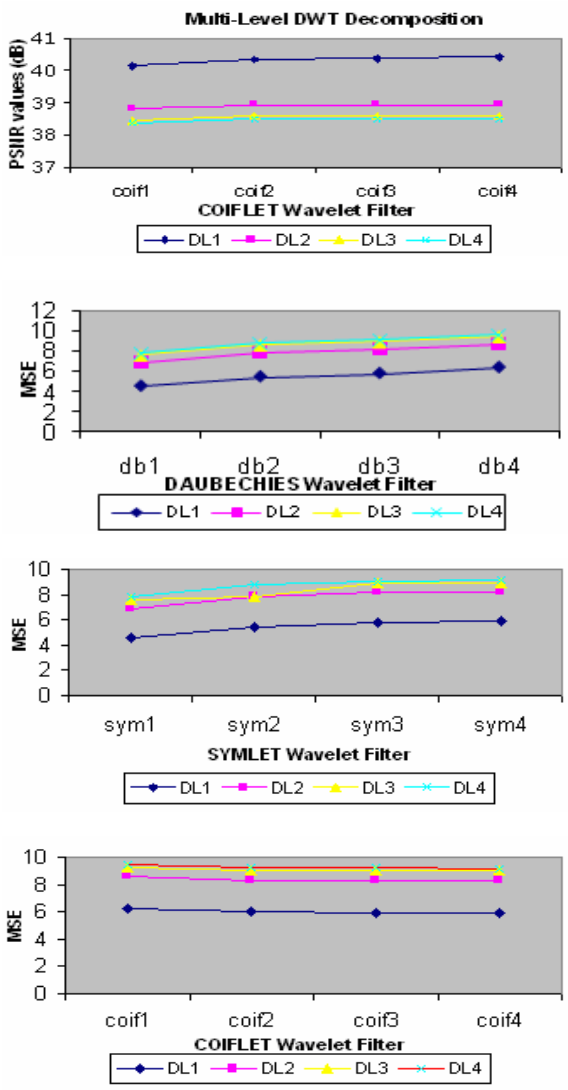

Figure 8. Graphical representations of PSNR and MSE values using multi-level DWT decomposition with wavelet filters.

Table 1. Total computational time of DWT decomposition using mother wavelets

Image slag	Time taken by DWT decomposition level 1	Time taken by DWT decomposition level 4
db1	0.6708 s	0.6786 s
sym1	0.6864 s	0.6903 s
bior6.8	0.6513 s	0.7371 s
coif4	0.6581 s	0.8541 s

4. Conclusion

In industry, welding plays a vital role in any component fabrication. The defects may occur in the weldment during this welding or in its lifetime. To secure safety and quality, the weldment must be tested. To do that, the advanced ultrasonic testing technique which has better probability of detection for defects is used. A major irritant during application of ToFD especially for testing of austenitic stainless steel weldments is the presence of noise. This noise must be suppressed to identify the defects in the welded components. To do that B-scan image is acquired using ultrasonic ToFD technique and also de-noised using discrete wavelet transform with various wavelet filters. The results are analyzed. The PSNR values of the wavelet filters db1, sym1, coif4 and bior6.8 are high at DWT decomposition level 1 whereas the MSE values get low for the same. Irrespective of the decomposition levels, PSNR values get decreased for daubechies and symlet wavelet filters with high vanishing moments whereas MSE values get increased for the same.

Irrespective of the decomposition levels, PSNR values get increased for biorthogonal and coiflet wavelet filters with high vanishing moments whereas MSE values get decreased for the same. Irrespective of wavelet filters, the image can be de-noised using multi-level DWT decompositions. The PSNR values of the de-noised image get decreased when the DWT decomposition level is increased and MSE gets increased for the same. It is concluded that the PSNR values get high only in low-level DWT

decomposition, i.e., good noise suppressed image can be obtained using low-level DWT decomposition with less computational cost.

Acknowledgements

The authors would like to thank the members of both the Central Workshop Division and UT Lab of Quality Assurance Division in IGCAR for their support for getting the experiments conducted.

The authors also thank the anonymous referees for their valuable suggestions which let to the improvement of the manuscript.

References

[1] Anutam and Rajni, Performance analysis of image denoising with wavelet thresholding methods for different levels of decomposition, Inter. J. Multimedia & Its Applications (IJMA) 6(3) (2014), 35-46.

[2] K. Manjula, K. Vijayarekha, B. Venkatraman and Durga Karthik, Ultrasonic time of flight diffraction technique for weld defects: a review, Res. J. Appl. Sci. Eng. Tech. 4(24) (2012), 5525-5533.

[3] Angam Praveen, Nikhilesh, K. Vijayarekha, K. Manjula and B. Venkatraman, Wavelet analysis and de-noising of signal, Res. J. Appl. Sci. Eng. Tech. 4(24) (2012), 5534-5538.

[4] K. Manjula, K. Vijayarekha and B. Venkatraman, Weld flaw detection using various ultrasonic techniques: a review, J. Appl. Sci. 14(14) (2014), 1529-1535.

[5] K. Manjula, K. Vijayarekha and B. Venkatraman, Noise reduction in ultrasonic signal for identification of weld defects: a review, Res. J. Appl. Sci. Eng. Tech. 6(24) (2013), 4595-4601.

[6] A. N. Sinclair, J. Fortin, B. Shakibi, F. Honarvar, M. Jastrzebski and M. D. C. Moles, Enhancement of ultrasonic images for sizing of defects by time-of-flight diffraction, NDT E International 43 (2010), 258-264.

[7] P. S. Hiremath, Prema T. Akkasaligar and Sharan Badiger, Visual enhancement of digital ultrasound images using multiscale wavelet domain, Pattern Recognition and Image Analysis 20(3) (2010), 303-315.